Supplemental Material

Supplemental Discussion

Gain and loss of functional connections in the H-DytRP network

As part of the study, we mapped individual functional connections that linked H-DytRP nodes in the MAN, NM, and SPOR groups but not in HC. Abnormal gain in connections linking the cerebellar vermis and hemispheres was observed in all three groups, supporting a major role for this structure in dystonia (Lerner et al., 2013; Quartarone and Hallett, 2013; Shakkottai et al., 2017; Quartarone et al., 2020). Certain connections were gained in dystonia gene carriers irrespective of penetrance, i.e., in both MAN and NM, such as those linking the Rolandic operculum with the putamen, and the inferior frontal operculum with the middle frontal gyrus. These abnormal connections were not detected in SPOR, suggesting that dystonic movements are mediated by other pathways in the latter group. That said, other functional connections were present in both MAN and SPOR but not in NM or HC, such as those linking the centromedian thalamus with the putamen, the Rolandic operculum with the angular gyrus, and the middle frontal gyrus with the precentral cortex. Of note, connectivity changes involving these regions have been reported previously in fMRI studies of focal dystonia (Battistella et al., 2017; Fuertinger and Simonyan, 2017). The delineation of abnormal functional connections such as these may help customize targets for therapeutic intervention in individual patients. Indeed, a recent deep brain stimulation (DBS) study found that cervical and generalized dystonia patients benefited clinically from distinct DBS stimulation pathways (Horn et al., 2022).

The study of H-DytRP connectivity in dystonia revealed parallels with recent data on the influence of genotype on the organization of Parkinson's disease networks. Specifically, in both

disorders, these effects were most pronounced in core subgraphs defined independently through community detection algorithms (Schindlbeck et al., 2020). Indeed, in MAN, prominent connectional gain was evident within the H-DytRP core, whereas in the other groups, this effect was greater outside this subgraph. The shift of the abnormal connections from the core in MAN to the periphery in SPOR may be clinically relevant. The H-DytRP periphery is composed largely of frontal, parietal, and occipital association regions, and the current data suggest a preponderance of such connections in SPOR patients. In hereditary dystonia, by contrast, connectional gain was more prominent in the core, linking cerebellar, thalamic, striatal, and motor cortical nodes within this module. As noted above, significant group differences in connectional loss were also observed in the core, but these were most pronounced in NM carriers as opposed to MAN and SPOR patients.

The meaning of the loss of normal connections in dystonia is less clear. It is tempting to associate reductions in functional connectivity as seen in the core zone of NM with microstructural changes in the integrity of thalamic outflow pathways to the motor cortex and striatum (Argyelan et al., 2009; Uluğ et al., 2011). The prominent loss of functional connections linking these core regions is therefore consistent with earlier DTI studies conducted in DYT1/DYT6 carriers which demonstrated a close relationship (Lerner et al., 2013; Vo et al., 2015). Of note, prominent loss of functional connectivity was also present in MAN and SPOR, but unlike NM, these changes were predominantly observed outside the core zone. For example, functional connections in the H-DytRP periphery linked the inferior frontal operculum (BA 44) and the angular gyrus (BA 39) in healthy subjects but were not present in either of the two

affected groups. Given that activity in these regions was anticorrelated in healthy individuals, it is possible that this projection normally has an inhibitory function that is lost in dystonia patients. Even so, one cannot determine from the rs-fMRI data alone whether the underlying anatomical connections are intact but functionally deactivated through interactions with other involved nodes or subnetworks, or alternatively whether the two regions are anatomically disconnected on a neurodevelopmental basis. DTI tractography can help disambiguate these possibilities. In this case, we observed a substantial reduction in the number of fiber tracts connecting these regions in MAN compared to HC subjects (Fujita et al., 2018). It is possible that similar changes underlie deficits in higher order functions such as sequence learning and visual motion perception reported in dystonia patients (Carbon et al., 2011; Sako et al., 2015; Fujita et al., 2018). Further multimodal imaging studies with rs-fMRI and DTI will be needed to evaluate these and other non-motor manifestations of the disorder.

References

Argyelan M, Carbon M, Niethammer M, Uluğ AM, Voss HU, Bressman SB, Dhawan V, Eidelberg D (2009) Cerebellothalamocortical connectivity regulates penetrance in dystonia. J Neurosci 29:9740–9747.

Battistella G, Termsarasab P, Ramdhani RA, Fuertinger S, Simonyan K (2017) Isolated Focal Dystonia as a Disorder of Large-Scale Functional Networks. Cereb Cortex 27:1203–1215.

Carbon M, Argyelan M, Ghilardi MF, Mattis P, Dhawan V, Bressman S, Eidelberg D (2011) Impaired sequence learning in dystonia mutation carriers: A genotypic effect. Brain 134:1416–1427.

Fuertinger S, Simonyan K (2017) Connectome-wide phenotypical and genotypical associations

in focal dystonia. J Neurosci 37:7438–7449.

Fujita K, Sako W, Vo A, Bressman SB, Eidelberg D (2018) Disruption of network for visual perception of natural motion in primary dystonia. Hum Brain Mapp 39:1163–1174.

Horn A et al. (2022) Optimal deep brain stimulation sites and networks for cervical vs. generalized dystonia. Proc Natl Acad Sci U S A 119:e2114985119.

Lerner RP, Niethammer M, Eidelberg D (2013) Understanding the anatomy of dystonia: Determinants of penetrance and phenotype. Curr Neurol Neurosci Rep 13:401.

Quartarone A, Cacciola A, Milardi D, Ghilardi MF, Calamuneri A, Chillemi G, Anastasi G, Rothwell J (2020) New insights into cortico-basal-cerebellar connectome: Clinical and physiological considerations. Brain 143:396–406.

Quartarone A, Hallett M (2013) Emerging concepts in the physiological basis of dystonia. Mov Disord 28:958–967.

Sako W, Fujita K, Vo A, Rucker JC, Rizzo JR, Niethammer M, Carbon M, Bressman SB, Uluı AM, Eidelberg D (2015) The visual perception of natural motion: Abnormal task-related neural activity in DYT1 dystonia. Brain 138:3598–3609.

Schindlbeck KA, Vo A, Nguyen N, Tang CC, Niethammer M, Dhawan V, Brandt V, Saunders-Pullman R, Bressman SB, Eidelberg D (2020) LRRK2 and GBA Variants Exert Distinct Influences on Parkinson's Disease-Specific Metabolic Networks. Cereb Cortex 30:2867–2878.

Shakkottai VG et al. (2017) Current Opinions and Areas of Consensus on the Role of the Cerebellum in Dystonia. Cerebellum 16:577–594.

Uluğ AM, Vo A, Argyelan M, Tanabe L, Schiffer WK, Dewey S, Dauer WT, Eidelberg D (2011) Cerebellothalamocortical pathway abnormalities in torsinA DYT1 knock-in mice.

Proc Natl Acad Sci U S A 108:6638–6643.

Vo A, Sako W, Niethammer M, Carbon M, Bressman SB, Ulug AM, Eidelberg D (2015) Thalamocortical connectivity correlates with phenotypic variability in dystonia. Cereb Cortex 25:3086–3094.

Supplemental Figures

Figure S1

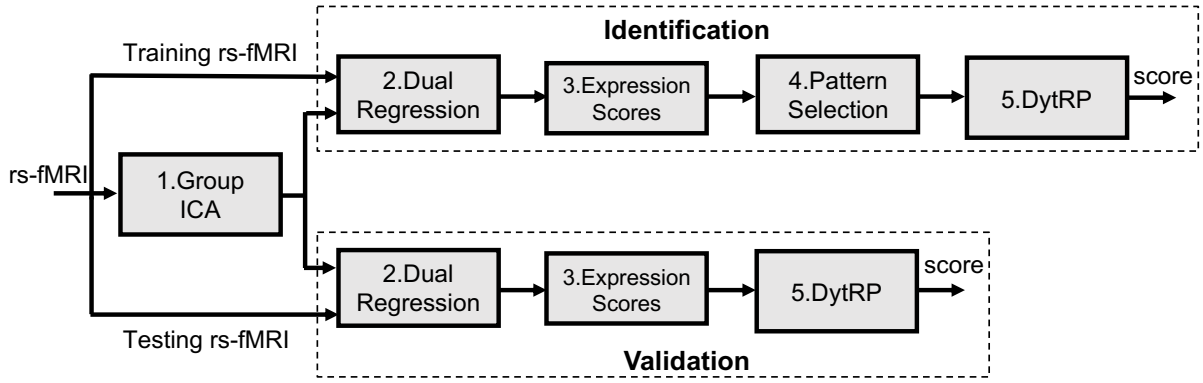

Figure S1. Identification and validation of dystonia-related pattern. For the identification of disease-related pattern, rs-fMRI scan data from dystonia patients and healthy control subjects were analyzed using spatial ICA to generate maps of the independent components (ICs) for both groups. Dual regression was applied to the individual scan data to compute subject scores for each of the group ICs. The dystonia disease-related pattern (DytRP) was defined as a linear combination of the smaller subset of group ICs selected using logistic regression analysis and bootstrap resampling (1000 iterations) of the subject scores (**Fig. 1** and **Fig. S3**). Validation of the DytRP into rs-fMRI scan data from individual subjects, we used dual regression to compute subject scores for the relevant group ICs. The resulting scores for each subject were linearly combined according to the estimated model coefficients to yield a composite DytRP expression value for that individual.

Figure S2

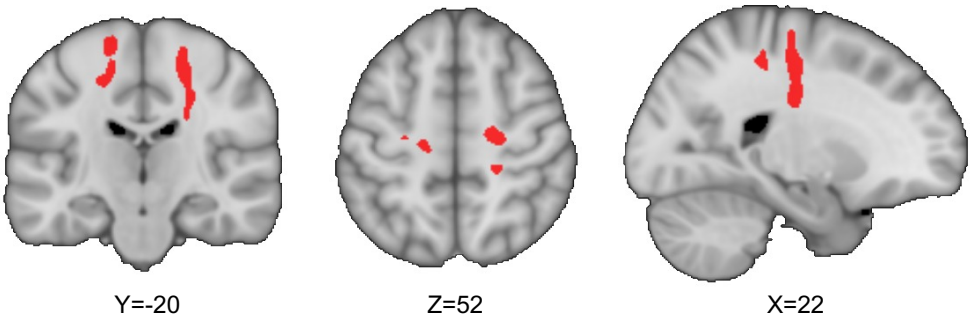

Figure S2. Subrolandic white matter (SWM) volume-of-interest identified in a voxel-wise analysis of FA maps from an independent set of MAN and NM DYT1/DYT6 carriers and HC subjects (see Methods). This volume was defined by significant bilateral FA reductions (*red voxels*) in NM compared to either MAN or HC.

Figure S3

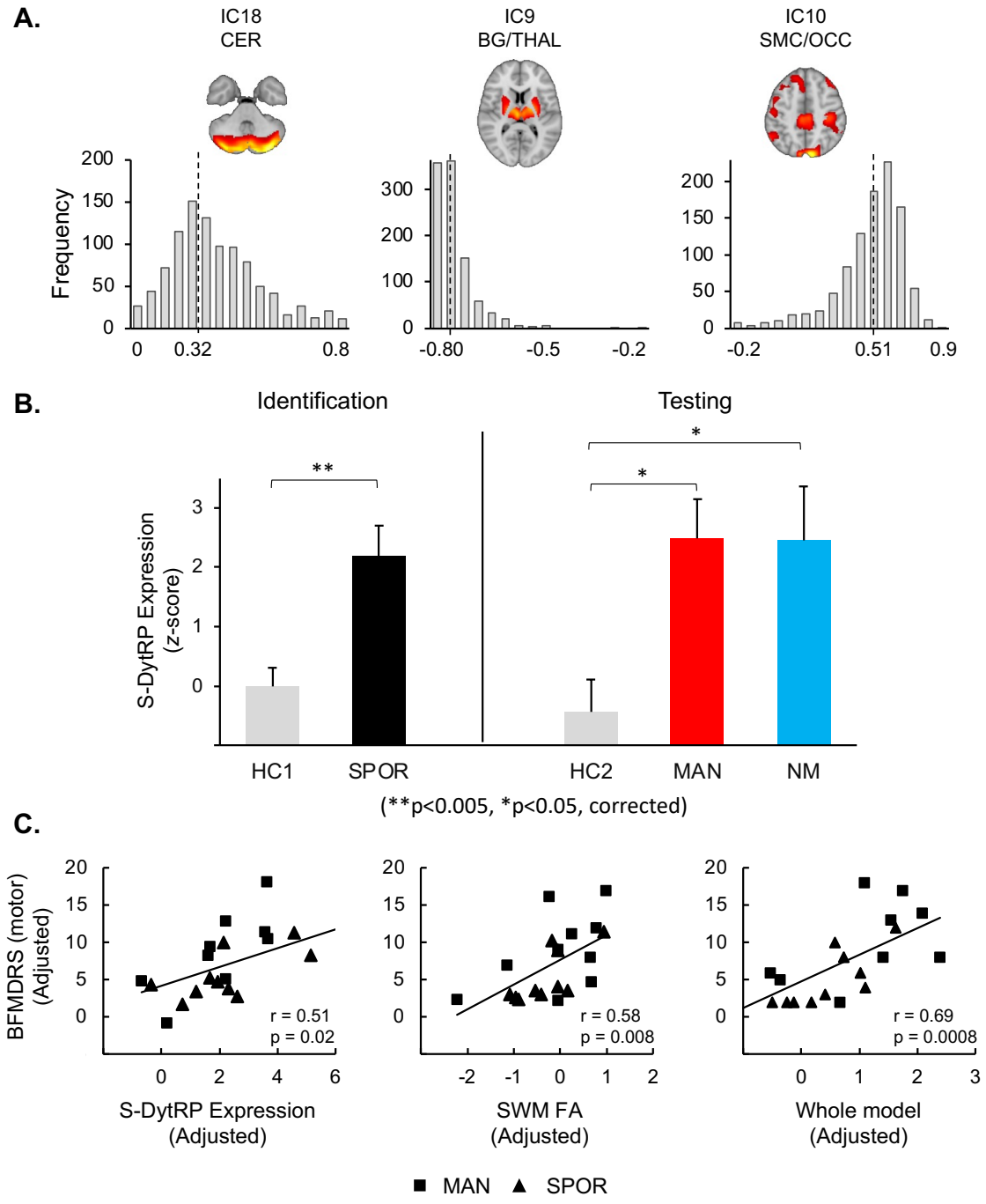

Figure S3. Sporadic dystonia-related pattern (S-DytRP). (A) Frequency histograms of the estimated weights on each of the selected independent components (ICs) based on bootstrap resampling (1000 iterations). In each iteration, we computed the weights on the individuals ICs

such that a linear combination of the associated subject scores accurately discriminated the patients from the healthy control subjects. The resulting weights formed a distribution for each of the ICs (*bottom row*), with the corresponding mean values (*vertical dashed lines*) denoting the respective coefficients (0.32, −0.80, and 0.51 for IC18, IC9, and IC10, respectively) on the composite S-DytRP network. The same coefficients were used prospectively to compute corresponding expression values (subject scores) for the S-DytRP in individual subjects (see Methods). [For each IC, key regions are displayed on representative MRI slices (*top row*). CER = cerebellum; BG/THAL = basal ganglia/thalamus; SMC/OCC = sensorimotor/occipital association cortex.] **(B)** *Left*: Expression scores for S-DytRP were elevated in the sporadic dystonia (SPOR) compared to the healthy control (HC1) subjects. *Right*: Significant increases in network expression were also seen in the manifesting dystonia (MAN) patients and non-manifesting (NM) gene carriers compared to HC2 testing subjects. **(C)** Clinical correlates of network expression. *Left*, *middle*: Partial correlation leverage plots of S-DytRP expression levels (rs-fMRI) and FA values (DTI) measured in a prespecified subrolandic white matter (SWM) volume-of-interest (**Fig. S2**; see Methods) to predict BFMDRS dystonia motor ratings obtained at the time of imaging. *Right*: A 2-predictor model based on both S-DytRP expression and SWM FA was superior to 1-predictor models based on either variable alone (see text). [BFMDRS = Burke–Fahn–Marsden Dystonia Rating Scale; rs-fMRI = resting-state functional magnetic resonance imaging; DTI = diffusion tensor imaging.]

Supplemental Tables

Table S1. Sample characteristics of the dystonia cohorts

	MAN (n=10)	NM (n=10)	SPOR (n=10)	HC1 (n=10)	HC2 (n=10)
Age (y)	43.3 ± 15.6	46.4 ± 16.9	46.3±17.3	46.7 ± 9.0	48.5 ± 6.6
Gender (M/F)	4/6	4/6	5/5	4/6	5/5
BFMDRS (motor)	9.2 ± 6.0	-	5.1 ± 3.7	-	-
Absolute displacement[a]	0.22 ± 0.12	0.28 ± 0.27	0.28 ± 0.40	0.25 ± 0.11	0.22 ± 0.11
Relative displacement[a]	0.10 ± 0.04	0.11 ± 0.10	0.10 ± 0.07	0.09 ± 0.03	0.08 ± 0.03

Means and standard deviations are shown for age in years (y), Burke-Fahn-Marsden Dystonia Rating Scale (BFMDRS) and motion displacement (mm). Sporadic dystonia (SPOR), manifesting (MAN) and non-manifesting (NM) carriers of *DYT1* or *DYT6* dystonia mutations, and healthy control (HC) subjects.
[a] Motion displacement (mm).

Table S2A. H-DytRP connections present in manifesting dystonia gene carriers but not healthy control subjects

MAN	Node 1 (AAL)	Node 2 (AAL)	HC[a]	MAN[b]	|*dr*|[c]
Core-Core	**Cerebellum_R (92)**	**Lingual_L (47)**	-0.32	0.79	1.11
	Cerebellum_R (92)	**Rolandic_Oper_L (17)**	-0.27	0.60	0.88
	Vermis (93)	**Rolandic_Oper_L (17)**	-0.22	0.73	0.96
	Thalamus_R (78)	**Putamen_R (74)**	0.19	0.89	0.70
	Thalamus_R (78)	**Rolandic_Oper_R (18)**	0.08	0.68	0.60
	Rolandic_Oper_L (17)	**Putamen_L (73)**	-0.26	0.72	0.98
	Rolandic_Oper_R (18)	**Putamen_R (74)**	0.18	0.78	0.60
	Rolandic_Oper_L (17)	**Lingual_L (47)**	0.22	0.64	0.42
Core-Periphery	**Vermis (93)**	Cerebellum_L (91)	0.19	0.78	0.60
	Rolandic_Oper_L (17)	Pons_L (94)	-0.12	0.60	0.73
	Angular_R (66)	**Putamen_R (74)**	-0.05	0.67	0.72
	Frontal_Mid_R (8)	**Pallidum_R (76)**	-0.12	-0.65	0.53
	Rolandic_Oper_L (17)	Angular_L (65)	-0.30	0.68	0.98
	Rolandic_Oper_R (18)	Angular_R (66)	-0.13	0.65	0.78
	Frontal_Inf_Oper_L (11)	Frontal_Mid_L (7)	-0.06	0.77	0.83
	Frontal_Mid_L (7)	**Precentral_L (1)**	0.06	0.88	0.82
Periphery-Periphery	Frontal_Inf_Oper_R (12)	Pons_R (95)	-0.01	-0.63	0.62
	Frontal_Mid_L (7)	Postcentral_L (57)	-0.10	0.65	0.75

[a],[b] The median r-value determined from 100 bootstrap iterations for the HC and MAN groups, respectively.
[c] The absolute difference (|*dr*|) computed for MAN relative to HC (see Methods).
Blue indicates gained connections in MAN that were also identified in NM (**Table S3A**). Red indicates gained connections in MAN that were also identified in SPOR (**Table S4A**). Green indicates connections gained in all three groups. Core nodes are signified by **bold** type.

Table S2B. H-DytRP connections present in healthy control subjects but not manifesting dystonia gene carriers

MAN	Node 1 (AAL)	Node 2 (AAL)	HC[a]	MAN[b]	$\|dr\|$[c]
Core-Core	**Putamen_L (73)**	**Pallidum_L (75)**	0.87	0.40	0.47
Core-Periphery	**Vermis (93)**	Frontal_Mid_R (8)	-0.70	0.28	0.98
	Pons_L (94)	**Vermis (93)**	-0.62	0.52	1.14
	Lingual_L (47)	Pons_L (94)	-0.80	0.50	1.30
	Angular_R (66)	**Lingual_R (48)**	0.66	0.11	0.55
	Frontal_Mid_R (8)	**Lingual_R (48)**	-0.76	-0.08	0.68
	Paracentral_Lobule_L (69)	**Precentral_L (1)**	0.79	-0.46	1.25
	Supp_Motor_Area_L (19)	**Precentral_L (1)**	0.82	0.07	0.76
Periphery-Periphery	Frontal_Inf_Oper_R (12)	Temporal_Pole_Sup_R (84)	0.78	0.16	0.62
	Frontal_Inf_Oper_R (12)	Angular_R (66)	-0.65	0.27	0.92
	Postcentral_L (57)	Paracentral_Lobule_L (69)	0.60	-0.37	0.98

[a],[b] The median r-value determined from 100 bootstrap iterations for the HC and MAN groups, respectively.
[c] The absolute difference ($|dr|$) computed for MAN relative to HC (see Methods).
Blue indicates connections in HC that were lost in both MAN and NM (**Table S3B**). Red indicates those lost in both MAN and SPOR (**Table S4B**). Green indicates healthy connections that were lost in all three groups. Core nodes are signified by **bold** type.

Table S3A. H-DytRP connections present in non-manifesting dystonia gene carriers but not healthy control subjects

NM	Node 1 (AAL)	Node 2 (AAL)	HC[a]	NM[b]	|*dr*|[c]
Core-Core	**Rolandic_Oper_L (17)**	**Putamen_L (73)**	-0.26	0.66	0.92
	Rolandic_Oper_R (18)	**Putamen_R (74)**	0.18	0.74	0.56
Core-Periphery	**Vermis (93)**	Cerebellum_L (91)	0.19	0.72	0.53
	Vermis (93)	Precentral_R (2)	-0.59	0.66	1.24
	Cerebellum_R (92)	Precentral_R (2)	0.00	0.66	0.66
	Vermis (93)	Paracentral_Lobule_R (70)	0.33	0.73	0.40
	Vermis (93)	Paracentral_Lobule_L (69)	-0.24	0.65	0.89
	Frontal_Inf_Oper_L (11)	Frontal_Mid_L (7)	-0.06	0.78	0.85
Periphery-Periphery	Cerebellum_L (91)	Precentral_R (2)	0.24	0.87	0.63

[a],[b] The median r-value determined from 100 bootstrap iterations for the HC and NM groups, respectively.
[c] The absolute difference (|*dr*|) computed for NM relative to HC (see Methods).
Blue indicates gained connections in NM that were also identified in MAN (**Table S2A**). Green indicates connections gained in all three groups. Core nodes are signified by **bold** type.

Table S3B. H-DytRP connections present in healthy control subjects but not non-manifesting dystonia gene carriers

NM	Node 1 (AAL)	Node 2 (AAL)	HC[a]	NM[b]	$\|dr\|$[c]
Core-Core	**Vermis (93)**	**Putamen_R (74)**	0.64	-0.01	0.65
	Thalamus_L (77)	**Putamen_L (73)**	-0.61	-0.01	0.61
	Pallidum_L (75)	**Thalamus_L (77)**	0.68	-0.19	0.87
	Rolandic_Oper_L (17)	**Pallidum_L (75)**	-0.61	0.40	1.02
	Precentral_L (1)	**Pallidum_L (75)**	-0.61	0.44	1.05
	Precentral_L (1)	**Rolandic_Oper_L (17)**	0.72	0.17	0.55
Core-Periphery	Cerebelum_L (91)	**Putamen_R (74)**	-0.62	0.06	0.68
	Frontal_Inf_Oper_R (12)	**Cerebelum_R (92)**	-0.66	0.20	0.87
	Frontal_Mid_R (8)	**Cerebelum_R (92)**	-0.79	-0.27	0.52
	Frontal_Inf_Oper_R (12)	**Vermis (93)**	-0.80	0.13	0.93
	Thalamus_R (78)	Fusiform_R (56)	0.73	0.25	0.48
	Thalamus_R (78)	Angular_R (66)	0.79	0.11	0.69
	Angular_R (66)	**Lingual_R (48)**	0.66	-0.36	1.02
	Precentral_L (1)	Paracentral_Lobule_L (69)	0.79	0.26	0.53
Periphery-Periphery	Frontal_Inf_Oper_R (12)	Temporal_Pole_Sup_R (84)	0.78	0.15	0.63
	Frontal_Mid_R (8)	Fusiform_R (56)	-0.69	-0.26	0.43
	Frontal_Mid_R (8)	Frontal_Inf_Oper_R (12)	0.84	0.35	0.48
	Supp_Motor_Area_R (20)	Precentral_R (2)	0.79	0.34	0.45
	Paracentral_Lobule_L (69)	Supp_Motor_Area_L (19)	0.95	0.44	0.50

[a],[b] The median r-value determined from 100 bootstrap iterations for the HC and NM groups, respectively.
[c] The absolute difference ($|dr|$) computed for NM relative to HC (see Methods).
Blue indicates connections in HC that were lost in both NM and MAN (**Table S2B**). Green indicates healthy connections that were lost in all three groups. Core nodes are signified by **bold** type.

Table S4A. H-DytRP connections present in sporadic dystonia patients but not healthy control subjects

SPOR	Node 1 (AAL)	Node 2 (AAL)	HC[a]	SPOR[b]	$\|dr\|$[c]
Core-Core	**Cerebellum_R (92)**	**Putamen_L (73)**	0.24	-0.85	1.10
	Cerebellum_R (92)	**Thalamus_L (77)**	0.29	-0.75	1.04
	Thalamus_R (78)	**Putamen_R (74)**	0.19	0.69	0.50
	Rolandic_Oper_R (18)	**Pallidum_R (76)**	-0.10	-0.66	0.56
	Rolandic_Oper_R (18)	**Lingual_R (48)**	0.04	0.63	0.59
Core-Periphery	Cerebellum_L (91)	**Vermis (93)**	0.19	0.66	0.47
	Cerebellum_R (92)	Fusiform_L (55)	-0.31	-0.90	0.59
	Vermis (93)	Paracentral_Lobule_L (69)	-0.24	0.63	0.87
	Vermis (93)	Paracentral_Lobule_R (70)	0.33	0.79	0.46
	Vermis (93)	Supp_Motor_Area_L (19)	-0.47	0.66	1.13
	Vermis (93)	Supp_Motor_Area_R (20)	-0.49	0.77	1.26
	Fusiform_L (55)	**Putamen_L (73)**	0.22	0.69	0.48
	Rolandic_Oper_R (18)	Pons_R (95)	0.04	-0.71	0.75
	Paracentral_Lobule_L (69)	**Lingual_L (47)**	-0.21	0.65	0.87
	Supp_Motor_Area_L (19)	**Lingual_L (47)**	-0.24	0.64	0.87
	Supp_Motor_Area_R (20)	**Lingual_R (48)**	-0.41	0.68	1.08
	Rolandic_Oper_R (18)	Angular_R (66)	-0.13	0.66	0.79
	Frontal_Mid_L (7)	**Precentral_L (1)**	0.06	0.61	0.55
Periphery-Periphery	Frontal_Mid_R (8)	Pons_R (95)	-0.07	0.60	0.67
	Angular_R (66)	Fusiform_R (56)	0.34	0.77	0.43
	Postcentral_R (58)	Pons_R (95)	0.14	-0.64	0.77
	Paracentral_Lobule_L (69)	Pons_L (94)	0.15	-0.73	0.88
	Paracentral_Lobule_R (70)	Pons_R (95)	-0.10	-0.74	0.65
	Precentral_R (2)	Pons_R (95)	0.11	-0.64	0.75
	Supp_Motor_Area_R (20)	Pons_R (95)	0.24	-0.84	1.08
	Supp_Motor_Area_L (19)	Pons_L (94)	0.30	-0.67	0.97

[a],[b] The median r-value determined from 100 bootstrap iterations for the HC and SPOR groups, respectively.
[c] The absolute difference ($|dr|$) computed for SPOR relative to HC (see Methods).
Red indicates gained connections in SPOR that were also identified in MAN (**Table S2A**). Green indicates connections gained in all three groups. Core nodes are signified by **bold** type.

Table S4B. H-DytRP connections present in healthy control subjects but not sporadic dystonia patients

SPOR	Node 1 (AAL)	Node 2 (AAL)	HC[a]	SPOR[b]	$\|dr\|$[c]
Core-Core	**Vermis (93)**	**Putamen_R (74)**	-0.61	-0.02	0.60
	Pallidum_L (75)	**Precentral_L (1)**	-0.61	0.00	0.61
	Pallidum_L (75)	**Rolandic_Oper_L (17)**	-0.61	0.19	0.80
Core-Periphery	**Vermis (93)**	Frontal_Inf_Oper_R (12)	-0.80	0.06	0.85
	Thalamus_R (78)	Angular_R (66)	0.79	0.28	0.51
	Thalamus_R (78)	Frontal_Mid_R (8)	-0.82	0.30	1.11
	Thalamus_R (78)	Fusiform_R (56)	0.73	0.27	0.46
	Frontal_Mid_R (8)	**Lingual_R (48)**	-0.76	-0.21	0.54
	Supp_Motor_Area_L (19)	**Precentral_L (1)**	0.82	0.11	0.72
Periphery-Periphery	Fusiform_R (56)	Pons_R (95)	0.61	0.17	0.44
	Frontal_Inf_Oper_R (18)	Angular_R (66)	-0.65	0.26	0.91
	Frontal_Inf_Oper_R (18)	Temporal_Pole_Sup_R (84)	0.78	-0.34	1.12
	Frontal_Mid_R (8)	Angular_R (66)	-0.63	0.10	0.73
	Frontal_Mid_R (8)	Frontal_Inf_Oper_R (12)	0.84	0.19	0.65
	Frontal_Mid_R (8)	Fusiform_R (56)	-0.69	0.13	0.82
	Supp_Motor_Area_R (20)	Angular_R (66)	-0.80	0.02	0.82

[a],[b] The median r-value determined from 100 bootstrap iterations for the HC and SPOR groups, respectively.
[c] The absolute difference ($|dr|$) computed for SPOR relative to HC (see Methods).
Red indicates connections in HC that were lost in both SPOR and MAN (**Table S2B**). Green indicates healthy connections that were lost in all three groups. Core nodes are signified by **bold** type.